(25) G. N. Schrauzer and E. Deutsch, *J. Am. Chem. Soc.*, **91**, 3341 (1969).
(26) T. Yamaguchi and T. Tsumura, *Chem. Lett.*, 409 (1973).
(27) H. O. House, "Modern Synthetic Reactions", W. A. Benjamin, New York, N.Y., 1968, p 164.
(28) R. L. Beach, *Tetrahedron Lett.*, 1913 (1972).
(29) I. S. Kolomnikov, V. P. Kukolev, and M. E. Vol'pin, *Russ. Chem. Rev.*, **43**, 399 (1974).
(30) The factorial experimental design is discussed in many books including (a) W. G. Cochran and G. M. Cox, "Experimental Designs", 2nd ed, Wiley, New York, N.Y., 1957; (b) O. Kempthorne, "The Design and Analysis of Experiments", Wiley, New York, N.Y., 1952; (c) W. J. Youden, "Statistical Methods for Chemists", Wiley, New York, N.Y., 1951; (d) E. L. Bauer, "A Statistical Manual for Chemists", 2nd ed, Academic Press, New York, N.Y., 1971.

Contribution from the Department of Chemistry,
University of Southern Mississippi, Hattiesburg, Mississippi 39401

Solvent Effects on the Coordination of Nd^{3+} in Concentrated $NdCl_3$ Solutions

MARCUS L. STEELE and DAVID L. WERTZ*

Received September 20, 1976 AIC607027

Nd^{3+} is, on the average, eight-coordinated in very concentrated solutions when anhydrous $NdCl_3$ is dissolved into 10 N hydrochloric acid or methanol as well as water. However, the extent to which $NdCl_3$ dissociates upon dissolution is dependent upon the solvent, with $NdCl(H_2O)_7^{2+}$, $NdCl_2(CH_3OH)_6^{+}$, and $Nd(H_2O)_8^{3+}$ being the average inner-sphere solute species in these three solutions. The inner-sphere Nd–O and Nd–Cl contact distances are ca. 2.41 and ca. 2.78 Å, respectively, and the ion-pair Nd···Cl distance is ca. 4.9 Å in each solution.

Introduction

In previous papers[1-5] it has been shown that lanthanide cations are, on the average, eight-coordinated in some concentrated solutions. These include solutions where the solvent is water and the solute is anhydrous LnX_3 (Ln = La, Nd, Gd; X = Cl, Br). In these aqueous solutions, $Ln(H_2O)_8^{3+}$ is the predominant solute species. However, extensive inner-sphere Ln–X bonding can occur when the solvent is methanol, and solute association appears to occur in an $LaCl_3$ solution.[3] Extensive Gd–Cl inner-sphere bonding also occurs in concentrated solutions where 10 N hydrochloric acid is the solvent;[2] but in an exactly equivalent solution where $LaCl_3$ is the solute, no inner-sphere La–Cl bonding occurs.[1]

Because differences in the extent of Ln–X inner-sphere bonding have been found in our previous investigations, we have examined two additional solutions of $NdCl_3$ with methanol and 10 N hydrochloric acid as solvents. The purpose of this investigation is to determine the following: (a) the coordination sphere details of the resulting solute complexes, (b) the extent to which Nd–Cl inner-sphere bonding occurs, (c) the extent to which Nd–Cl and/or Nd–O bonding is affected by the solvent, and (d) additional information for the development of a unifying theory regarding lanthanide–ligand interactions.

For each of the solutions examined, the mole fraction of Nd^{3+} is 0.010. The results of this investigation are compared to the results obtained from a similar study of aqueous $NdCl_3$ solutions. The solutions were examined by x-ray diffraction methods.

Experimental Section

Solutions were prepared by weight from predried anhydrous $NdCl_3$. Densities were measured with a specific gravity bulb. Solution compositions are shown in Table I, and for convenience one of the aqueous $NdCl_3$ solutions[4] is also included as solution C. Each solution was loaded into a Teflon sample holder, which had a window covered by a 1.0-mil Mylar film, and an x-ray diffraction pattern was obtained using the reflection method.[6] Scattered intensities were collected using our θ–θ diffractometer[2] as counts per preset time as a function of the scattering angle in the range $s = 1.23–15.09$ Å^{-1} ($s = 4\pi\lambda^{-1}\sin\theta$) at increments in θ of 0.25°. At least three runs over the entire angular range were made for each solution. The average intensity at each scattering point was used in subsequent calculations. For these solutions the maximum value of $\sigma < 1\%$,[7] and σ is significantly lower at most of the 219 data points at which data were collected.

Table I. Solution Compositions

	Solution		
	A	B	C
Solvent	10 N HCl	Methanol	Water
Molality	1.54	1.95	1.73
Density, g/L	1.29	1.08	1.26
Mole fractions			
Nd	0.010	0.010	0.010
Cl	0.060	0.030	0.030
O	0.300	0.160	0.320
H	0.630	0.640	0.640
C		0.160	

Table II. Summary of the ARDF'S

	Soln A	Soln B	Soln C
Peak location, Å			
C–O peak		1.48	
P1	2.49	2.56	2.41
P2	3.3	3.2	3.2
P3	4.1	4.1	3.8, 4.1
P4	4.8	4.9	4.5, 4.9
P5		5.6	6.2
P6	6.8	6.8	6.7
P7			
P8			
Area under 1st peak, e^2	101	119	83
Area/Nd^{3+}, e^2	10 100	11 900	8300
Width at half-maximum, Å	0.46	0.54	0.36

The scattered intensity was corrected for background (ca. 5 cpm), polarization,[8] sample penetration,[9] multiple scattering,[10] and, after inclusion of a monochromator discrimination function, Compton scattering.[11] The corrected intensity, e.g., the coherent intensity curve $I(s)$, was then tentatively computer fitted to $\sum x_i f_i^2(s)$,[12] according to the methods of Lawrence and Kruh.[13] Final fitting of $I(s)$ to $\sum x_i f_i^2(s)$ was performed by a method similar to that used by Konnert and Karle.[14] Atomic radial distribution functions (ARDF's) were calculated at increments in Δr of 0.01 and 0.05 Å by

$$D(r) = 4\pi r^2\rho_0 + (2r/\pi)\int [si(s)]\,[M(s)]\,[\sin sr]\;ds$$

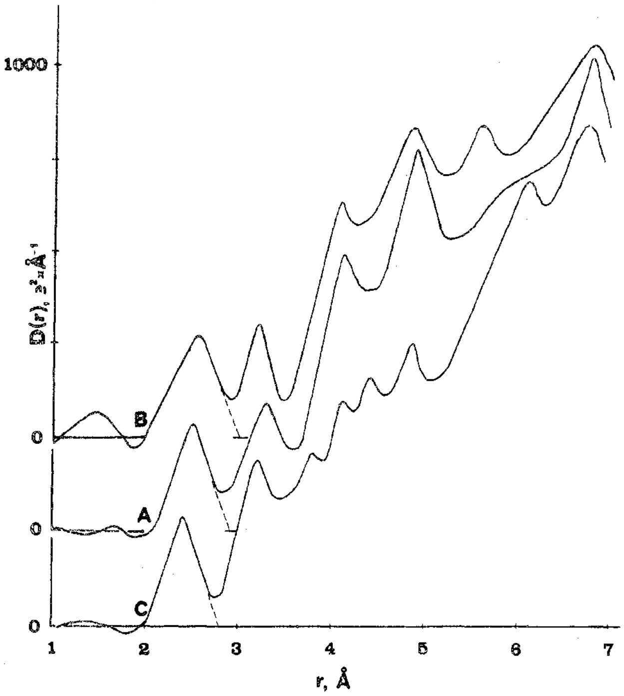

Figure 1. ARDF's of the $NdCl_3$ solutions with $x_{Nd} = 0.010$: A, in 10 N hydrochloric acid; B, in methanol; C, in water.

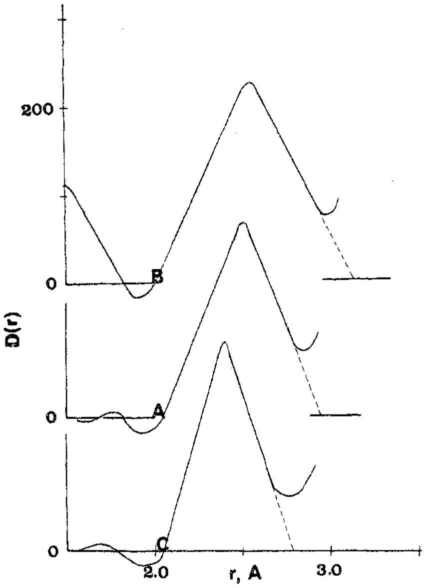

Figure 2. Enlargement of the ARDF's in the region of the first peak.

With this method $D(r)$ provides a weighted measure of the probability of finding atom pairs in the solution separated by a distance between r and $r + dr$, ρ_0 is the bulk density of the solution, $si(s) = s[I_{coh}(s) - \sum x_i f_i^2(s)]$, and

$$M(s) = \{\Sigma x_i f_i(0)/\Sigma x_i f_i(s)\}^2\{\exp(-bs^2)\}\mathrm{USF}$$

USF is a unit step function which terminates the integral at $s_{max} = 15$ Å^{-1}.

Shown in Figure 1 are the ARDF's obtained with $b = 0.010$. The ARDF's are summarized in Table II. An enlargement of P1 for each ARDF is shown in Figure 2.

The area under the first peak in each ARDF was determined via repeated graphical integration so that deviation from the mean area of each first peak was <2% of the peak area.

For each solution the ideal peaks anticipated for one Nd–O atom pair and for one Nd–Cl atom pair per Nd^{3+} were calculated by

$$T_{Nd-O}(\mu) = (x_{Nd}/\pi)\int f_{Nd}f_O[M(s)](\cos \mu s)\, ds$$

Table III. The Ideal Peaks

Nd–O Peak		Nd–Cl Peak	
μ, Å	$T(\mu)$, e^2 Å^{-1}	μ, Å	$T(\mu)$, e^2 Å^{-1}
0.0	34.7	0.0	92.1
0.1	28.3	0.1	72.2
0.2	13.6	0.2	27.5
0.3	0.5	0.3	−0.3
0.4	−4.7	0.4	−15.9
0.5	−3.1	0.5	−14.4
0.6	−0.3	0.6	−1.1
0.7	1.1	0.7	6.3
0.8	−1.2	0.8	1.4
0.9	1.6	0.9	−2.3
1.0	−0.5	1.0	1.2
1.1	0.7	1.1	4.0
1.2	0.6	1.2	3.0
1.3	−0.4	1.3	−0.3
1.4	−0.6	1.4	−1.5
1.5	0.1	1.5	0.2
1.6	0.7	1.6	2.0
1.7	0.5	1.7	1.4
1.8	−0.2	1.8	−0.7
1.9	−0.4	1.9	−1.3
2.0	0.1	2.0	0.2

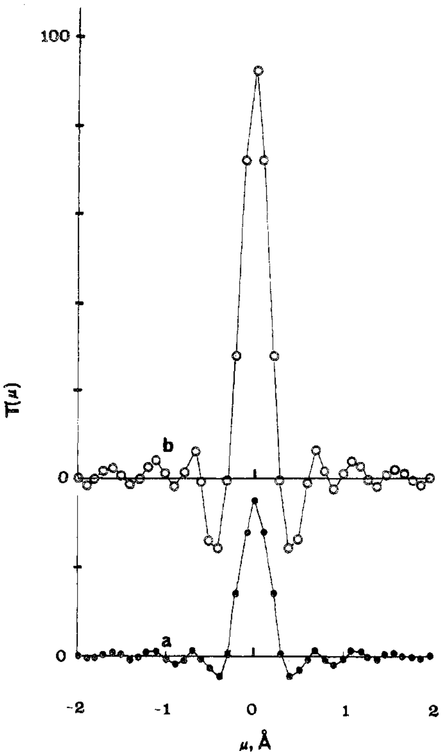

Figure 3. Ideal peaks calculated for (a) an Nd–O atom pair and (b) an Nd–Cl atom pair for solution A.

and

$$T_{Nd-Cl}(\mu) = (x_{Nd}/\pi)\int f_{Nd}f_{Cl}[M(s)](\cos \mu s)\, ds^{15}$$

In these equations μ is the distance from the maximum of the ideal peak and the $f_i(s)$ are the scattering factors. Shown in Table III are $T_{Nd-O}(\mu)$ and $T_{Nd-Cl}(\mu)$ for these solutions, and shown in Figure 3 are graphical representations of T_{Nd-O} and T_{Nd-Cl}. The ideal peak area for each ideal peak may be determined by integrating $T(\mu)$ between the limits of $\mu_{min} = -2.00$ Å and $\mu_{max} = 2.00$ Å. Thus, $A^*_{Nd-O} = \int T_{Nd-O}(\mu)\, d\mu$ and $A^*_{Nd-Cl} = \int T_{Nd-Cl}(\mu)\, d\mu$. A^*_{Nd-O} and A^*_{Nd-Cl} were determined, by repeated graphical integration, to be 10.4 and 28.0 e^2, respectively.

The contribution that each atom pair is anticipated to make to the area per Nd^{3+} may be calculated by $A_{Nd-O} = A^*_{Nd-O}/x_{Nd^{3+}}$ and $A_{Nd-Cl} = A^*_{Nd-Cl}/x_{Nd^{3+}}$; or $A_{Nd-O} \simeq 1040$ e^2 and $A_{Nd-Cl} \simeq 2800$ e^2; i.e., each Nd–O atom pair contributes ca. 1040 e^2 and each Nd–Cl atom pair

Table IV. Primary Peak Correlations

Soln	n_1[a]	I,[b] e^2	n_2	II,[c] e^2	Σ(I + II), e^2	Area/Nd^{3+},[d] e^2
A	7.0	7280	1.0	2800	10 080	10 100
B	6.0	6240	2.0	5600	11 840	11 900
C	8.0	8320	0.0	0	8 320	8 300

[a] The uncertainty in calculating n_{Nd-O} and n_{Nd-Cl} is ca. ±3%. [b] Contribution to the area/Nd^{3+} from inner-sphere Nd-O interactions; i.e., $I = n_1 A_{Nd-O}$. [c] Contribution to the area/Nd^{3+} from inner-sphere Nd-Cl interactions; i.e., $II = n_2 A_{Nd-Cl}$. [d] The area/Nd^{3+} has been determined, via repeated graphical integration, to a precision of ±3% from integrating P1 in each ARDF.

contributes ca. 2800 e^2 to the area per Nd^{3+}.

Both the position of and the area under the first peak have been utilized to determine the average inner-sphere coordination of Nd^{3+} in each solution by

$$P1 \simeq (n - n_2 + n_2 Q)^{-1}(n_1 d_{Nd-O} + n_2 Q d_{Nd-Cl}) \qquad (1)$$

and

$$P1A = n_1(1040\ e^2) + n_2(2800\ e^2) \qquad (2)$$

In these equations, n_1 and n_2 are the average number of Nd–O and Nd–Cl contacts per Nd^{3+}, d_{Nd-X_i} are the Nd–O and Nd–Cl distances as determined in crystals, $Q \simeq A_{Nd-Cl}/A_{Nd-O}$, P1 is the location of the first peak, and P1A is the area under the peak in each ARDF. For these solutions, the average coordination number of Nd^{3+} is n; i.e., $n = \sum n_1 + n_2$.

Based upon this method of correlating the primary peak in the ARDF with the average inner-sphere coordination of a cation, the uncertainty in the determination of the coordination number of the cation is not significantly larger than the uncertainty in the area under the primary peak. In several other solutions,[16] the maximum uncertainty in the coordination number of the cation appears to be less than 0.2, and this is consistent with error estimates by Konnert and Karle.[14]

Results and Discussion

The C–O Peak. The ARDF of solution B contains a peak at about 1.48 Å. This peak is due to the C–O interaction characteristic of methanol,[17] the solvent in this solution. The peak is not present in the ARDF's of solutions A and C.

The Primary Peak. As the solvent changes, the location and the width at half-maximum of the first peak and the area per Nd^{3+} change perceptibly, as is shown in Table II as well as in the ARDF's. However, the remaining portions of the ARDF's are similar. Such changes in the details of the first peak indicate that the average inner-sphere coordination features of Nd^{3+} are affected by the solvent and may be interpreted as either changes in the inner-sphere coordination number or changes in the occupation of the inner-sphere ligand sites (or both).

As noted in our study of the concentrated aqueous $NdCl_3$ solutions,[4] the average inner-sphere solute species is $Nd(H_2O)_8{}^{3+}$. This species is consistent with an area per Nd^{3+} of ca. 8300 e^2 and an average Nd–O distance of ca. 2.41 Å (solution C).

If the areas per Nd^{3+} observed in the ARDF's of solutions A and B are correlated only with Nd–O inner-sphere bonding ($n_2 = 0$), then the average inner-sphere solute species would be ca. $Nd(H_2O)_{10}{}^{3+}$ in solution A and ca. $Nd(ROH)_{12}{}^{3+}$ in solution B. Both species are unreasonable.

On the other hand, chloride occupation of the inner coordination sphere is usually increased when the solvent is changed from water to 10 N hydrochloric acid[2,18,19] or to methanol,[3,20] and in no case is an increase in the inner-sphere coordination number reported. Thus as an alternate model, it has been assumed that $n = 8$ for all three solutions and that $n_2 \neq 0$ for solutions A and B. Via eq 2, n_1 and n_2 have been estimated; and the results are shown in Table IV. Thus with this model the average inner-sphere solute species are ca. $NdCl(H_2O)_7{}^{2+}$ in solution A and ca. $NdCl_2(CH_3OH)_6{}^{+}$ in solution B. The shift in the maximum and the broadening of P1 as well as the area per Nd^{3+} are consistent with the latter model. However, repeated attempts to resolve the inner-sphere Nd–O peak from the Nd–Cl peak in the ARDF's of solutions A and B have been unsuccessful. This is not surprising since the M–O peak and the M–Cl peak have not been resolved in the ARDF's of several other aqueous solutions of metal chloride salts.

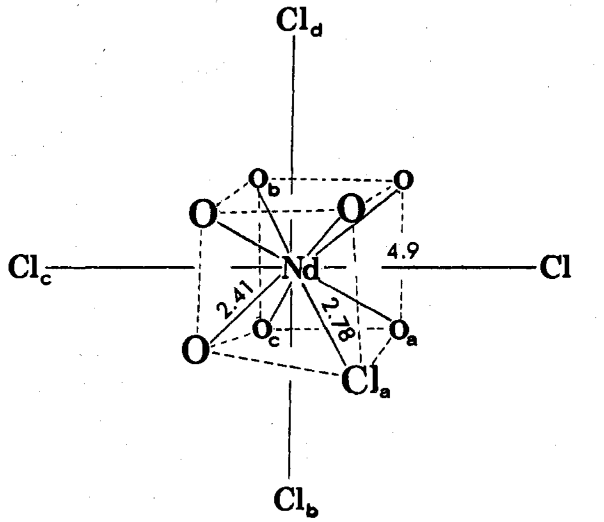

Figure 4. Solute model of $ClNd(H_2O)_7{}^{2+}$ which is consistent with the ARDF of solution A. The pertinent Nd–ligand distances are indicated.

In the aqueous $NdCl_3$ solutions, the average Nd–O inner-sphere distance is 2.41 Å. Consequently, it has been assumed that the inner-sphere Nd–O distance is 2.41 Å in each solute complex. By utilizing this bond distance and the values of n_1 and n_2 determined above, the inner-sphere Nd–Cl distance has been estimated via eq 1. This distance is estimated to be 2.78 Å in solution A and 2.79 Å in solution B. The consistency of these values and the close agreement between these calculated values and $\sum(r_{Nd^{3+}} + r_{Cl^-}) = 2.80$ Å indicate that the values of n_1 and n_2 chosen and the eight-coordinated inner-sphere model are consistent with the first peak in each ARDF.[21]

No other coordination model accounts for the change in location and the change in shape of P1 in a reasonable manner.

The Second Peak. In either aqueous or methanolic solutions which contain chloride, strong hydrogen bonding occurs. Such interactions occur at 3.1–3.2 Å when water[1,2,4,22–24] or methanol[3,20] is the solvent and at ca. 3.3 Å when hydrochloric acid[1,2,18,19] is the solvent. The ARDF of solution B exhibits a peak at 3.2 Å and the ARDF of solution A exhibits a peak at 3.3 Å. These peaks, due primarily if not exclusively to hydrogen-bonded Cl–O interactions, unfortunately mask other atom-pair interactions which could be utilized to evaluate various detailed solute coordination models. Consequently the existence of this peak in each ARDF cannot be utilized to evaluate various solute models.

The Fourth Peak. Ion-pair Ln···Cl interactions are found in the range 4.7–5.0 Å in the ARDF's of the $LnCl_3$ solutions previously studied.[1–4,24] These ARDF's contain a large peak at 4.9 Å (P4). The peak is due to ion-pair Nd···Cl interactions. In the ARDF's of the aqueous $NdCl_3$ solutions,[4] the ion-pair Nd···O interaction distance was identified at ca. 4.5 Å. However, in the ARDF's of solutions A and B, no perceptible peak at 4.5 Å appears; indicating that ion-pair Nd···O interactions are much less important in these two solutions than in the aqueous $NdCl_3$ solutions.

Table V. Summary of the Interactions of the Solute Model for $NdCl(H_2O)_7^+$

Atom pair	Calcd dist, Å	Peak in ARDF	Examples
Nd–O	2.41	1	Nd–O
Nd–Cl	2.78	1	$Nd–Cl_a$
Cl· · ·O	3.02	2	$Cl_a\cdot\cdot\cdot O_a$
Cl· · ·O	3.2–3.3	2	H-bonded Cl–O
O· · ·O	3.94	3	$O_a\cdot\cdot\cdot O_b$
O· · ·Cl[a]	4.02	3	$O_a\cdot\cdot\cdot Cl_b$
Cl· · ·Cl[a]	4.00	3	$Cl_a\cdot\cdot\cdot Cl_b$
Cl· · ·O	4.26	3	$Cl_a\cdot\cdot\cdot O_c$
Nd· · ·Cl[a]	4.9	4	$Nd\cdot\cdot\cdot Cl_c$
Cl· · ·O	5.12	4	$Cl_a\cdot\cdot\cdot O_b$
O· · ·Cl[a]	6.69	6	$O_a\cdot\cdot\cdot Cl_c$
Cl· · ·Cl[a]	6.91	6	$Cl_a\cdot\cdot\cdot Cl_c$
Cl· · ·Cl[a]	6.93	6	$Cl_b\cdot\cdot\cdot Cl_c$

[a] These interactions depend upon chlorides occupying the outer-sphere sites, as depicted in Figure 2.

Speculations Regarding the Remaining Peaks. On the basis of our solute model, it is possible to account for all of the peaks in the ARDF of solution A. It has been assumed with this model of the solute species that the inner ligand sheath is "cubic" and that the second coordination polyhedron is "octahedral". Because the peak at 4.9 Å is quite large in the ARDF of solution A and because the ion-pair Nd···O peak is not discernible, the "octahedral" second sheath is occupied principally by chlorides. The model is shown in Figure 4 and summarized in Table V. The principal feature of this model is that it readily predicts the peaks at 4.1 and at 6.8 Å, the former being primarily due to interactions between second-sphere chlorides and inner-sphere ligands and the latter being due both to interactions between outer-sphere ligands and to second sphere–inner sphere ligand interactions.

Any other coordination model predicts several additional peaks which are not seen in the ARDF of solution A and/or accounts for the peaks which are observed in the ARDF of solution A. Consequently this model must be viewed as a plausible description of the solute species in solution A.

A similar model accounts for all of the peaks observed in the ARDF of solution B except peak 5, particularly if the second inner-sphere chloride replaces O_b (Figure 4). This peak occurs at $2d_{Nd-Cl}$ and may be attributed to the trans nonbonded Cl···Cl interaction, though other atom-pair interactions could contribute as well. The model also accounts for the ARDF's of the aqueous $NdCl_3$ solutions.

Conclusions

X-ray diffraction experiments clearly establish that the occupation of ligand sites but not the average coordination number of Nd^{3+} is affected by changing solvent conditions when the solute is $NdCl_3$ and the solutions are very concentrated. In each of the $NdCl_3$ solutions examined, Nd^{3+} has, on the average, eight nearest neighbors. The average species are $NdCl(H_2O)_7^{2+}$, $NdCl_2(CH_3OH)_6^+$, and $Nd(H_2O)_8^{3+}$ when the solvents are 10 N hydrochloric acid, methanol, and water, respectively. The Nd–O and Nd–Cl bond distances are ca. 2.41 and ca. 2.78 Å, respectively, while the ion-pair Nd···Cl distance is ca. 4.9 Å.

A model of the solute species where Nd^{3+} is surrounded, on the average, by a pseudocubic inner-coordination sheath of ligands and a pseudooctahedral second ligand coordination sphere is consistent with the ARDF's of the $NdCl_3$ solutions where water and 10 N hydrochloric acid are the solvents. The model, in each case, describes the ARDF's obtained with a high degree of precision.

Chloroheptaaquoneodymium(III), the average species found in the hydrochloric acid solution, is intermediate between octaaquolanthanum(III) and dichlorohexaaquogadolinium(III), the species found in comparable $LaCl_3$ and $GdCl_3$ solutions.[1,2] This result suggests that the extent to which nearest-neighbor Ln–Cl bonds occur parallels the increasing potential of the various lanthanides and/or their 4f-orbital electron occupation.

No evidence of solute association is found in the methanolic $NdCl_3$ solution.

Acknowledgment. The support of a Frederick R. Cottrell grant from the Research Corp. is gratefully acknowledged.

Registry No. $NdCl(H_2O)_7^{2+}$, 62006-73-9; $NdCl_2(CH_3OH)_6^+$, 62029-59-8; $Nd(H_2O)_8^{3+}$, 62006-59-1; Nd^{3+}, 14913-52-1; $NdCl_3$, 10024-93-8.

References and Notes

(1) L. S. Smith and D. L. Wertz, *J. Am. Chem. Soc.*, **97**, 2365 (1975).
(2) M. L. Steele and D. L. Wertz, *J. Am. Chem. Soc.*, **98**, 4424 (1976).
(3) L. S. Smith, D. C. McCain, and D. L. Wertz, *J. Am. Chem. Soc.*, **98**, 5125 (1976).
(4) M. L. Steele and D. L. Wertz, *J. Am. Chem. Soc.*, in press.
(5) L. S. Smith and D. L. Wertz, *J. Inorg. Nucl. Chem.*, **39**, 95 (1977).
(6) H. A. Levy, M. D. Danford, and A. H. Narten, Report ORNL-3960, Oak Ridge National Laboratory, Oak Ridge, Tenn., 1966.
(7) σ = (total counts)$^{-1/2}$ × 100 at each data point.
(8) B. D. Cullity, "Elements of X-ray Diffraction", Addison-Wesley, Reading, Mass., 1956, p 172.
(9) A. H. Narten and H. A. Levy, *Science*, **165**, 447 (1969).
(10) B. E. Warren, "X-ray Diffraction", Addison-Wesley, Reading, Mass., 1969, p 145.
(11) F. Hajdu, *Acta Crystallogr., Sect. A*, **27**, 73 (1971); F. Hajdu and G. Palinkas, private correspondence.
(12) F. Hajdu, *Acta Crystallogr., Sect. A*, **28**, 250 (1972).
(13) R. M. Lawrence and R. F. Kruh, *J. Chem. Phys.*, **41**, 4758 (1967).
(14) J. H. Konnert and J. Karle, *Acta Crystallogr., Sect. A*, **29**, 702 (1973).
(15) J. Waser and V. Schomaker, *Rev. Mod. Phys.*, **25**, 671 (1953).
(16) D. L. Wertz and J. R. Bell, *J. Inorg. Nucl. Chem.*, **35**, 861 (1973).
(17) D. L. Wertz and R. F. Kruh, *J. Chem. Phys.*, **47**, 388 (1967).
(18) D. L. Wertz and J. R. Bell, *J. Inorg. Nucl. Chem.*, **35**, 137 (1973).
(19) J. L. Tyvoll and D. L. Wertz, *J. Inorg. Nucl. Chem.*, **36**, 3713 (1974).
(20) D. L. Wertz and R. F. Kruh, *J. Chem. Phys.*, **50**, 4013, 4313 (1969).
(21) F. A. Cotton and G. Wilkinson, "Advanced Inorganic Chemistry. A Comprehensive Text", Interscience, New York, N.Y., 1972, pp 52, 1057.
(22) J. R. Bell, J. L. Tyvoll, and D. L. Wertz, *J. Chem. Soc.*, **95**, 1456 (1973).
(23) J. N. Albright, *J. Chem. Phys.*, **56**, 3783 (1972).
(24) G. W. Brady, *J. Chem. Phys.*, **33**, 1079 (1960).